

MIPAS IN-FLIGHT CALIBRATION AND PROCESSOR VERIFICATION

H. Nett⁽¹⁾, G. Perron⁽²⁾, M. Sanchez⁽¹⁾, A. Burgess⁽¹⁾, P. Mosner⁽³⁾

⁽¹⁾ ESTEC (EOP-PPP), P.O. Box 299, NL-2200 AG Noordwijk, e-mail: hnett/msanchez/aburgess@estec.esa.nl

⁽²⁾ ABB BOMEM Inc., 585 Charest E., Quebec, Qc, Canada G1K 9H4, e-mail: gaetan.p.perron@ca.abb.com

⁽³⁾ Astrium GmbH, D-81663 München, e-mail: peter.mosner@astrium-space.com

ABSTRACT

The Michelson Interferometer for Passive Atmospheric Sounding is one of the atmospheric payload instruments on board ESA's ENVISAT which was successfully launched into a sun-synchronous, polar orbit on 1 March 2002. Covering a broad spectral range from 685 - 2410 cm^{-1} , at high spectral resolution and radiometric sensitivity the instrument permits unprecedented observations of a large number of atmospheric trace gases from the upper Troposphere up into the Meso-sphere. Throughout its expected lifetime of 4.5 years systematic processing and dissemination of MIPAS products is envisaged which cover both fully calibrated, geo-located limb radiances (Level 1B) and vertical profiles of atmospheric pressure, temperature and volume-mixing-ratios of the primary target species O_3 , H_2O , CH_4 , N_2O , NO_2 and HNO_3 (Level 2).

During the initial 9 month period of in-orbit operation an extensive program of calibration and validation activities have been carried out. The analysis of the acquired measurement data confirmed excellent performance with regard to spectral stability, radiometric performance and line-of-sight (LOS) pointing accuracy. This paper summarises primary results of MIPAS data analyses completed by the data of the ENVISAT Calibration Review, held from 9 - 13 September 2002.

1 INTRODUCTION

MIPAS has been designed to acquire global measurements of the Earth's limb emission in an altitude range from approx. 6 km to 68 km. Based on the Fourier transform measurement technique it provides coverage of a broad spectral range, from 685 - 2410 cm^{-1} ($\lambda = 14.6 \dots 4.15 \mu\text{m}$), at simultaneously high spectral resolution (0.03 cm^{-1}) it allows to detect and spectrally analyse numerous middle atmospheric gases, of which O_3 , H_2O , CH_4 , N_2O , HNO_3 , and NO_2 have been selected as primary target species ([1], [2]). The Envisat ground segment concept foresees systematic processing and dissemination of calibrated, geo-located limb radiance spectra (Level 1B) as well as abundance profiles of the six target gases, along with atmospheric pressure (p), temperature (T), included in the Level 2 data products. During the initial four week's period after launch a couple of basic functional checks were successfully completed, during which the instrument's health and full commandability was verified. These activities were followed by dedicated calibration measurements, in order to establish a stable scene acquisition and calibration scenario and to verify critical elements of the on-ground data processing chain.

This paper shall provide an overview of MIPAS calibration tasks which have been completed so far and outline the role of the ESA external expert teams involved in the project. Results of in-flight performance analyses will be presented.

2 IN-ORBIT CALIBRATION & VERIFICATION TASKS AND TEAM ORGANISATION

The early MIPAS in-orbit functional checks and calibration / verification tasks can be grouped according to:

- **Switch-On and Data Acquisition Phase (SODAP)**
 - stabilisation of the thermal environment and basic checks of the instrument's functional components
 - unlocking and initial 'switch on' of telescope scan mechanisms, coolers, and of the interferometer slides
 - verification of the commandability in the different modes and of the communication between instrument, satellite and the flight operation segment
- **Initial instrument characterisation activities**
 - instrument related performance analysis, covering characterisation of radiometric noise, accuracy and non-linearity, spectral axis assignment, instrument lineshape (ILS), line-of-sight (LOS) mispointing
 - drift analyses and optimisation of calibration cycles (e.g., radiometric gain/offset calibrations, ILS retrievals)
 - acquisition of initial calibration data for use in Level 1B processing

- generation of a preliminary L1B data set for use in early Level 2 algorithm analyses
- identification and correction of potential inconsistencies in the Level 0 to 1B processing stage
- optimisation of instrument settings (PAW gains, ...)
- **full Level 1B related characterisation & validation**
 - update of in-flight characterisation parameters and generation of full set of Level 1B processor input data
 - optimisation of critical Level 1B algorithm components and settings
 - initialisation of routine performance monitoring functions, i.e., definition of settings used on ground for routine instrument health checks and to detect potential degradations with respect to the initial performance
 - assessment of total Level 1B error budgets including instrument and inaccuracies induced by the Level 1B ground processor and through inaccurate characterisation parameters.

The activities have been carried out in a co-ordinated effort and involve both, industrial and scientific expert teams. Table 1 summarises the instrument and Level 1B related tasks. A detailed outline of the MIPAS CalVal activities, and of the overall organisation of the CalVal team, is provided in [3].

Table 1. MIPAS calibration and algorithm verification activities

Involved institutes / companies	Task	Remarks
ABB BOMEM Inc., ASTRIUM GmbH, ESA/ENVISAT project team	<ul style="list-style-type: none"> • initial instrument health checks, switch-on and functional check-out • characterisation & optimisation of instrument parameters (e.g., analog & digital signal processing) • characterisation of performance parameters (detector non-linearity, NESR levels, radiometric accuracy, drifts in radiometric gain / offset data, ILS shape & stability, spectral axis linearity, ...) • characterisation of systematic LOS mispointing • optimisation of settings for routine calibration measurements (spectral resolution, repeat cycles for deep space calibration, ...) • generation of template data for L1B validation functions • initialisation of long-term performance monitoring functions • routine generation and maintenance of L1B auxiliary data bases 	Analysis performed using calibration chains installed on the MIPAS Calibration Processor (MICAL) installed at ESTEC
DLR-IMF, FZ-IMK, IAA	<p>Independent performance analyses:</p> <ul style="list-style-type: none"> • analysis of noise sources verification of NESR data reported in MIPAS L1B products • verification of detector non-linearity correction scheme implemented in MIPAS L1B algorithm by means of alternative analyses • Verification of ILS parametrisation as implemented in MICAL chain • Verification of ILS stability and characterisation of tangent altitude dependencies • spectral calibration analysis and characterisation of residual errors in L1B data • characterisation of spurious signals in deep space calibration measurements 	Work carried out in the frame of announcement of opportunity projects AO#145 (PI: Th.v. Clarmann); AO#652 (PI: M. Birk)
all teams	identification of potential errors in Level 1B algorithm and recommendations for enhancements of critical components and the auxiliary input data	
ABB BOMEM Inc., DJO GmbH	implementation & verification of Level 1B algorithm changes or auxiliary data enhancements as resulting from AO project and IECF activities	

3 DATA ACQUISITION

Since the initial instrument switch-on on 24 March 2002 MIPAS has been acquiring calibration and scene measurement data according to pre-defined scenarios. Level 0 products were generated at the receiving payload data handling station located in Kiruna/Sweden (PDHS-K) and nominally transmitted to the MIPAS calibration platform (MICAL), currently located at ESTEC. Depending on actual instrument mode, associated data rate and on the duration of specific acquisition segments the size of individual product files varies between ~ 900 KBytes and 290 MBytes. A total of ~ 120 GBytes of Level 0 data have been transferred and locally stored on the MICAL platform in period 24 March - 24 August, during which the bulk of the calibration / characterisation measurements were scheduled. This corresponds to approx. one third of the overall Level 0 data volume acquired by PDHS-K during that period (considering the daily ~ 10 Kiruna visibility

orbits only). Table 2 provides a summary of instrument modes, associated Level 0/1B products and data rates. Note that in case of scene and radiometric gain data processing in the PDS or MICAL also Level 1B data will be generated.

Table 2. Overview MIPAS measurement modes, data rates and products

instrument mode / activity	data rate	product	total no. of files	volume
MEASUREMENT (nom, sem, BB, DS)	305 ... 325 Kbits/s	MIP_NL__0P	795	118.6 GBytes
LOS	0.9...1.2 Kbits/s	MIP_LS__0P	213	17.2 MBytes
RAW, SPE Selftest	1.4...4.2 Mbits/s	MIP_RW__0P	11	1.23 GBytes
instrument mode / activity		product	typ. size (per orbit)	
MEASUREMENT (nom, sem, BB, DS)	-/-	MIP_NL__1P	295 MBytes	

4 MIPAS IN-FLIGHT PERFORMANCE

Performance specifications & in-flight verification

The planning of dedicated calibration / characterisation measurements and the analysis of acquired instrument data have been carried out in agreement with the MIPAS CalVal implementation plan ([3]). A detailed description of the actually applied processing algorithms is given in [4], [5].

Table 3 summarises main characteristics of MIPAS and performance specifications.

Table 3. MIPAS characteristics and performance specifications

Observation geometry	
Line-of-sight (LOS) geometry	LOS tangent height range: 68 km ... 6 km (nominal scenario) Pointing range (azimuth, relative to S/C velocity vector): 160 ⁰ - 190 ⁰ (rearward viewing) 75 ⁰ - 110 ⁰ (sideward viewing)
Instantaneous field-of-view (IFOV)	full FOV width: 0.0523 ⁰ (elevation) * 0.523 ⁰ (azimuth) At LOS tangent point (effective): 3 km (vertical)*30 km (horizontal)
horizontal sampling	displacement between subsequent elevation scan sequences (typ., rearward viewing): approx. 400 km
Spectral sampling & performance	
spectral range	685 - 2,410 cm ⁻¹
spectral band definition (contributing detectors in brackets)	A: 685-970 cm ⁻¹ (A1, A2) AB: 1,020-1,170 cm ⁻¹ (B1) B: 1,215-1,500 cm ⁻¹ (B2) C: 1,570-1,750 cm ⁻¹ (C1, C2) D: 1,820-2,410 cm ⁻¹ (D1, D2)
spectral resolution	0.035 cm ⁻¹ (unapodised, full resolution, MPD = 20 cm)
spectral linearity	better than 0.001 cm ⁻¹

Table 3. MIPAS characteristics and performance specifications

Spectral sampling & performance (continued)		
spectral stability	better than 0.001 cm^{-1} (for periods < 165 s)	
instrument lineshape (ILS)	secondary peak height: < 25 % of main peak lineshape area (squared ILS): area between FWHM points > 70 % [total area] stability: ILS variation: < 0.35 % (main peak amplitude) at any point over 5 days	
Radiometric performance		
noise equivalent spectral radiance for negligible input radiance (NESR_0)	band A (685 - 970 cm^{-1}): 50 nW / ($\text{cm}^2 \cdot \text{sr} \cdot \text{cm}^{-1}$) band AB (1020 - 1170 cm^{-1}): 40 nW / ($\text{cm}^2 \cdot \text{sr} \cdot \text{cm}^{-1}$) band B (1215 - 1500 cm^{-1}): 20 nW / ($\text{cm}^2 \cdot \text{sr} \cdot \text{cm}^{-1}$) band C (1570 - 1750 cm^{-1}): 20 nW / ($\text{cm}^2 \cdot \text{sr} \cdot \text{cm}^{-1}$) band D (1820 - 2410 cm^{-1}): 4.2 nW / ($\text{cm}^2 \cdot \text{sr} \cdot \text{cm}^{-1}$)	
radiometric accuracy	685 - 1,500 cm^{-1} : $2 * \text{NESR}_T + 5 \%$ [true source spectral radiance] 1,570 - 2,410 cm^{-1} : $2 * \text{NESR}_T + X \%$ of [true source spectral radiance] X to be linearly interpolated between 2 at 1,570 cm^{-1} and 3 at 2,410 cm^{-1} NESR_T : NESR when the instrument is viewing a blackbody source at temperature T	
dynamic range (blackbody source input)	(0 -230) K	
LOS mispointing		
Parameter	elevation	azimuth ^a
initial LOS acquisition (no LOS correction)	bias: 108 mdeg 1. harmonic: 25 mdeg	135 (total)
acquisition accuracy (with LOS correction)	40 mdeg	not specified
pointing knowledge (with LOS correction)	25.3 mdeg	
pointing stability (equivalent tangent height variation)	acquisition of a single spectrum ($\tau = 4 \text{ s}$) < 0.3 km^a acquisition of an elevation sequence ($\tau = 75 \text{ s}$) < 0.9 km^a	

a. no in-flight characterisation of azimuth mispointing envisaged

The results of the in-flight performance characterisation are summarised in the following sections.

4.1. Radiometric performance (IF8, IF10)

NESR₀:

The NESR_0 figures have been checked in all spectral bands and compared both to the specified values and to results of pre-flight performance tests based on the flight model instrument (FM). The results are shown in Figure 1 (a).

Observed noise levels are in general consistent with the pre-flight test results. Lower values compared to the FM result are found in band AB, which is probably linked to a change of the on-board undersampling ('decimation') factor used in that band.

Radiometric accuracy:

The radiometric accuracy has been checked for the calibration blackbody as input source, at a temperature of 230 K. In the scenario considered the drifts in the radiometric gain over a period of approx. 8 days has been taken into account (nominal gain calibration frequency: 7 days). The result is shown in Figure 1 (b). It should be noted that drifts in radiometric gain is probably dominated by water ice deposition on the instrument's focal plane sub-system (FPS), which results in a systematic drop of overall optical throughput with increasing time. It has been found that such contamination

effects can be reduced by warming up the FPS from the nominal temperature of 70 K to levels above 230 K over a period of a couple of days.

The currently found values for radiometric accuracy are within specifications for all bands. However, it should be noted that only a single level of the input radiance has been considered so far. Radiometric errors may increase for lower signal flux levels, in particular for bands A, AB and B, due to errors in detector non-linearity characterisation.

Further analyses of the overall radiometric performance are still in progress.

Figure 1 (a). In-flight characterised noise equivalent spectral radiance (NESR₀)

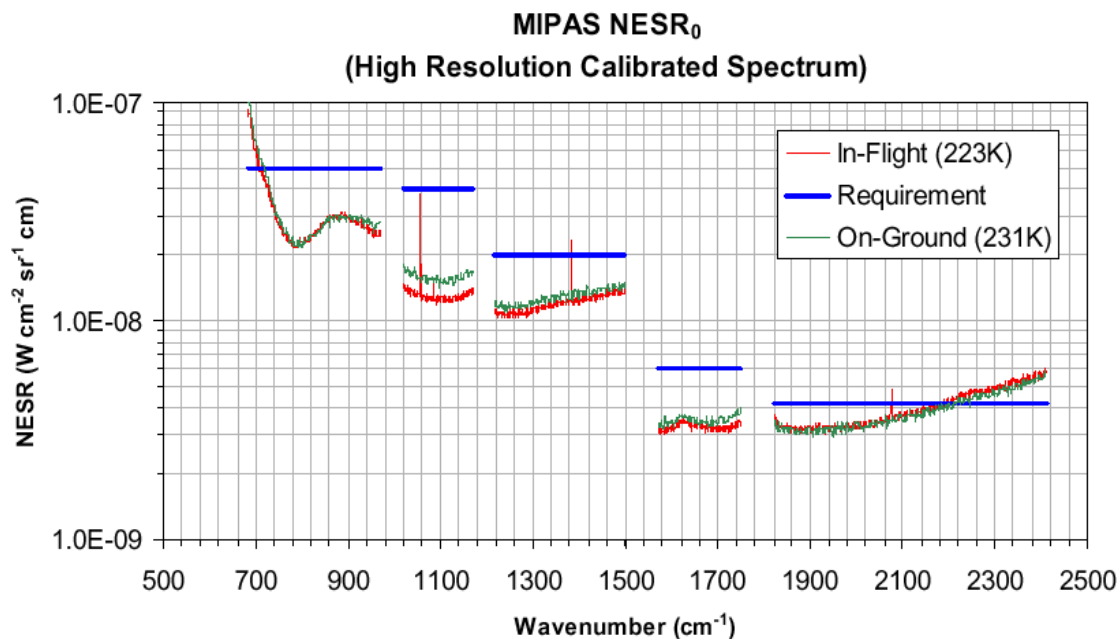
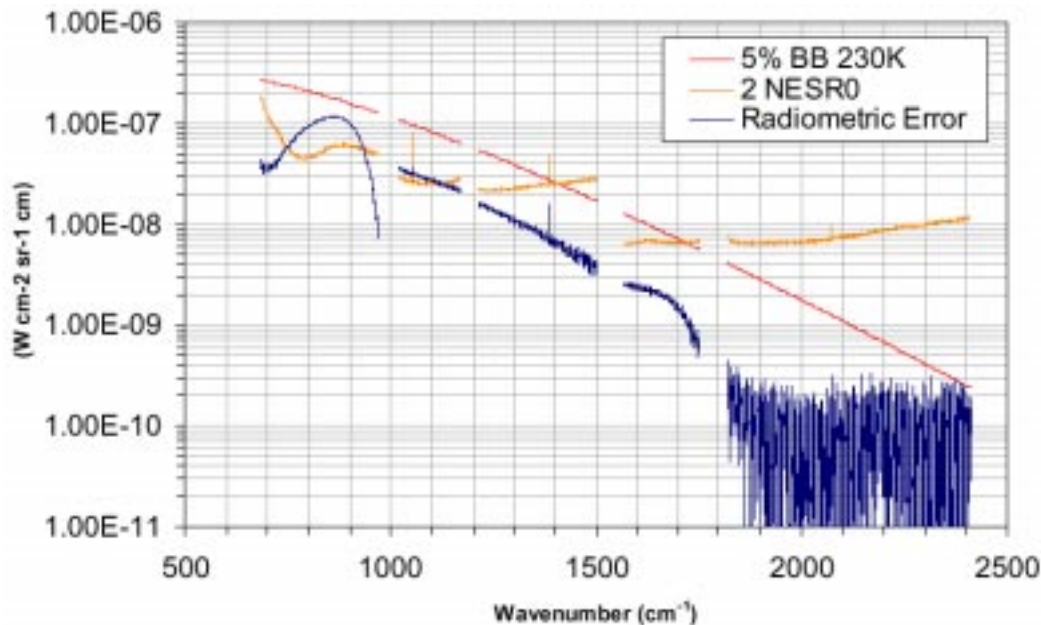


Figure 1 (b). Radiometric accuracy assessment (for calibration blackbody at 230 K)



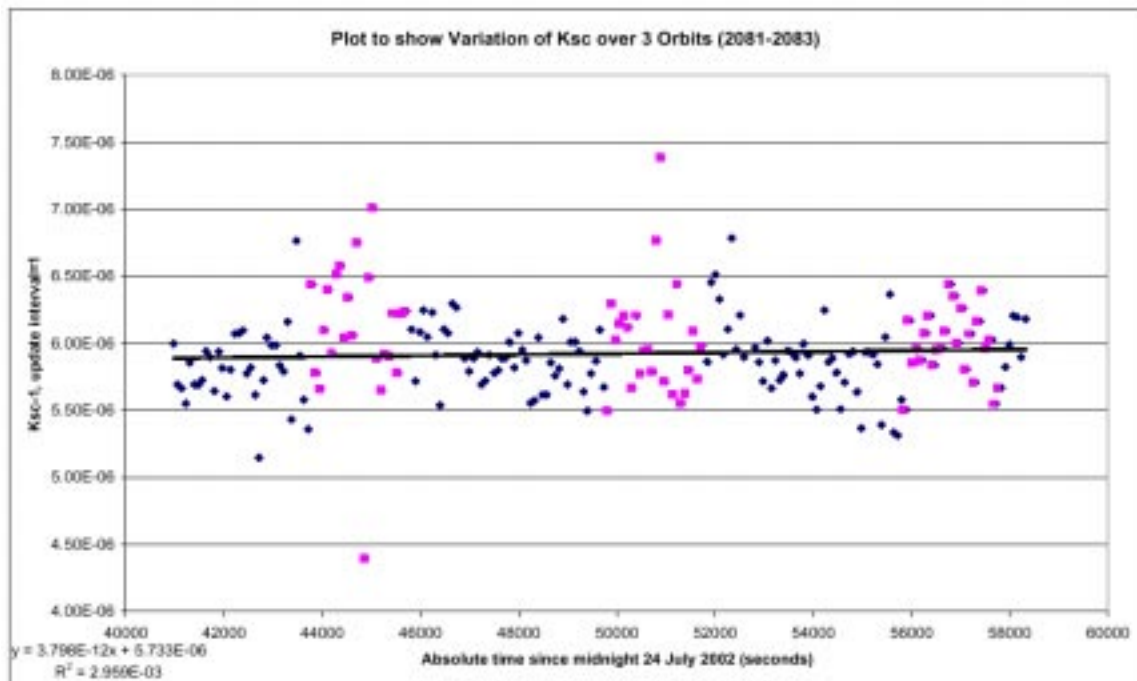
4.2. Spectral performance (IF2)

The strategy for in-flight spectral calibration and instrument lineshape retrievals, which is based on the analysis of well-known spectral signatures in the observed target atmosphere, has been subject of extensive tests. In particular, the impact of atmospheric scene variations and of spectral interference effects in the analysed frequency intervals ('microwindows') were found critical for the overall achievable accuracies and stability of results. An optimisation of various algorithm settings and, in particular, the choice of microwindows was considered necessary and has been successfully completed. The overall strategy adopted and a detailed discussion of the results are provided in [4], [5], [6].

A typical result is shown in Figure 2, which shows the variation of the linear spectral axis stretching factor (K_{sc}) over a period of approx. 3 full orbits. In the analysed scenario an independent K_{sc} value is determined for each individual elevation sequence (approx. 80 s), in order to investigate the impact of scene variations near the dusk/dawn boundaries for a nominal orbit scenario. Note that in a nominal spectral calibration scenario scene spectral are averaged over typically four elevation scans. This will enhance the achievable signal-to-noise ratios and thus reduce significantly the variations in computed K_{sc} values.

In summary, all performance parameters characterised in-flight were found within the specified values, after implementation of an enhanced set of microwindows for both spectral calibration and ILS retrievals. However, further optimisation of critical settings and a characterisation of long-term drifts in the retrieved results due to instrumental effects are still considered necessary.

Figure 2. Variations of in-flight retrieved spectral axis correction factors ($K_{sc} - 1$)



4.3. LOS mispointing characterisation (IF1)

The strategy for characterising systematic mispointing of the instrument's line-of-sight is based on the sensing of a set of suitable infrared-bright stars for typical periods of 1-2 orbits. Given precise information of platform position and attitude, the elevation/azimuth pointing angles of MIPAS and the position of the target object the expected entry / exit times of a star when crossing the field-of-view can be computed and compared to the measured signals. The actual delay for an individual star 'passage' is computed by means of a cross-correlation with a reference signal and can be converted into a mispointing parameter. A detailed description of the LOS calibration scheme and of the underlying processing algorithms is given in [8].

In the selected scenario a two orbit period was chosen (# 2622 and #2623, on 31 Aug. 2002), with a total of 61 IR star observations in rearward viewing geometries. Between 3 and 7 passages were commanded for each target by means of discrete stepping in the elevation direction, resulting in typical measurement durations between 16 s and 42 s. This multi-stepping approach allows co-addition of individual signals, in order to reduce the impact of detector / pre-amplifier noise. Figure 3 (a) shows a typical signal as acquired in detector channel D1. The output signal covers 7 passages in this example, each resembling a ‘derivative’ signal of the FOV pattern (a consequence of the AC coupling in the analogue signal processing and the constant apparent velocity of the star while crossing the FOV). Also visible are spurious signals which originate from the discrete stepping of the elevation scan unit. Figure 3 (b) shows the crosscorrelations of individual signals with a reference signal.

In the example shown a time shift of - 415 ms is detected which corresponds to a mispointing +24.9 mdeg with respect to the instrument’s pitch (X-) axis. The LOS misalignment is modelled by fitting simultaneously a bias and a first harmonic component for both the pitch and the roll axis by means of a non-linear least-squares fit analysis, using all available measurements in a given measurement sequence:

$$\Delta\text{pitch} = A_{0,\text{pitch}} + A_{1,\text{pitch}} * \cos(\omega_{\text{orb}} * t_{\text{anx}} - \Phi_{\text{pitch}})$$

$$\Delta\text{roll} = A_{0,\text{roll}} + A_{1,\text{roll}} * \cos(\omega_{\text{orb}} * t_{\text{anx}} - \Phi_{\text{roll}})$$

where $\omega_{\text{orb}} = 2 * \pi * T_{\text{orb}}$ ($T_{\text{orb}} = 6036$ s, the orbital period), t_{anx} the elapsed time since ascending node crossing and $(A_{0,\text{pitch}}, A_{1,\text{pitch}}, \Phi_{\text{pitch}})$ and $(A_{0,\text{roll}}, A_{1,\text{roll}}, \Phi_{\text{roll}})$ represent the unknowns to be fitted, i.e. bias + 1. harmonic component’s amplitude and phase for pitch and roll axes, respectively.

Figure 3. LOS signal acquisition in orbit # 2622, (IR source RAFGL4292, $t_{\text{anx}} = 1612$ s)

(a) raw signal in detector channel D1

(b) result of cross-correlation for individual star passages (before co-addition)

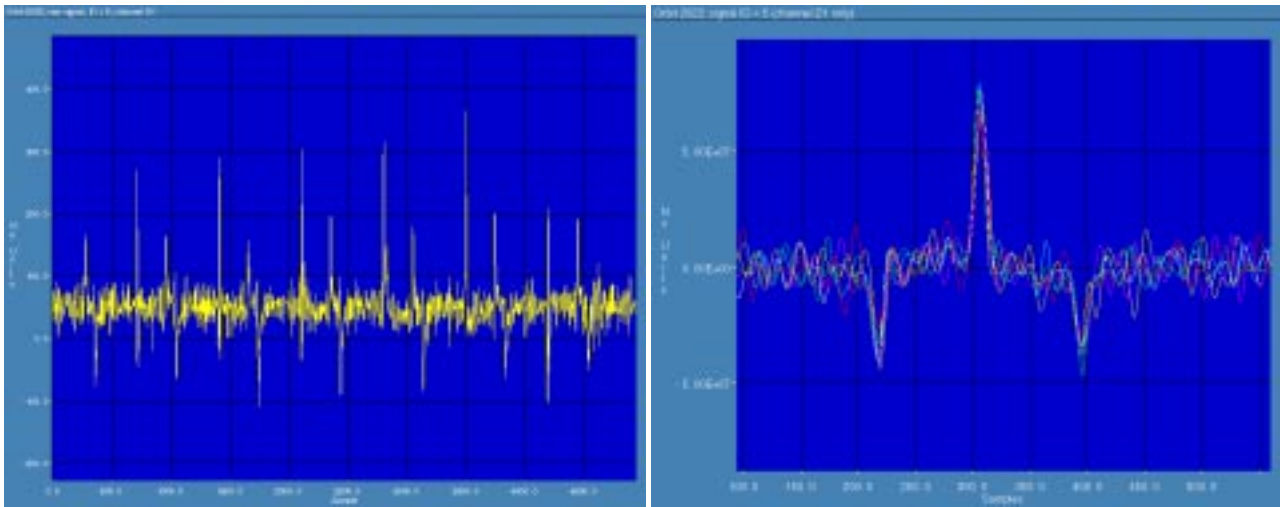


Table 4 summarises the results of the LOS misalignment analysis for the LOS acquisition performed in orbits 2622 & 2623.

Table 4. LOS mispointing analysis for orbits 2622&2623 (31 August 2002)

LOS analysis, orbits 2622 & 2623					
Axis	parameter		initial guess	NLS fit result (3 iterations)	
X (pitch)	$A_{0,pitch}$		+100 mdeg	$A_{0,pitch}$	+ 14.9 mdeg
	1. harmonic	cos	50 mdeg	$A_{1,pitch}$	13.0 mdeg
	1. harmonic	sin	20 mdeg	Φ_{pitch}	95.7 deg
Y (pitch)	$A_{0,roll}$		+100 mdeg	$A_{0,roll}$	- 4.9 mdeg
	1. harmonic	cos	50 mdeg	$A_{1,roll}$	0.9 mdeg
	1. harmonic	sin	20 mdeg	Φ_{roll}	-63.2 deg

The retrieved misalignment parameters for both the pitch and the roll axes are well within specifications reported in Table 2. However, the contributions of various systematic errors (e.g., misalignment characterisation data, errors in the commanded timelines, orbit propagation errors) still need to be assessed. Furthermore, the long-term stability of the results have to be characterised, in order to optimise the update frequency of the misalignment characterisation.

4.4. In-flight FOV checks (IF14)

The mispointing characterisation discussed in the previous section provides information on the absolute alignment of the instrument's line-of-sight with respect to the commanded elevation and azimuth angles, using detectors D1 and D2 as a reference. An other critical parameters is the relative misalignment of individual detector channels which had been subject to characterisation measurements with the FM prior to launch. It was found, however that the available measurement data provided only insufficient accuracy, in particular for the long-wavelength channels, A1, A2, B1, B2.

Figure 4 (a).

Measurement geometry for in-flight FOV check (IF14)

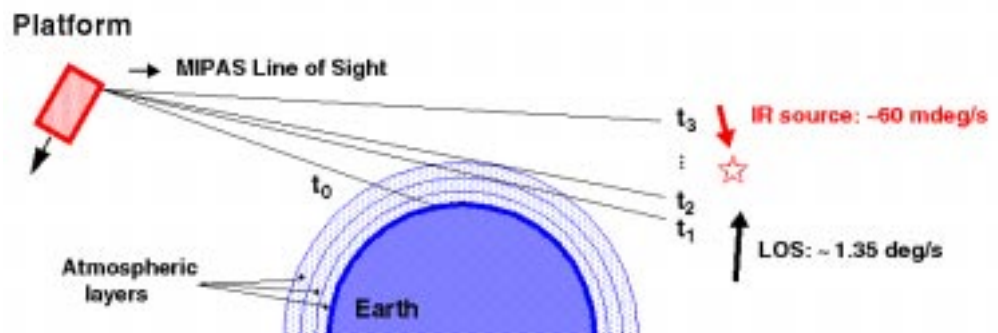
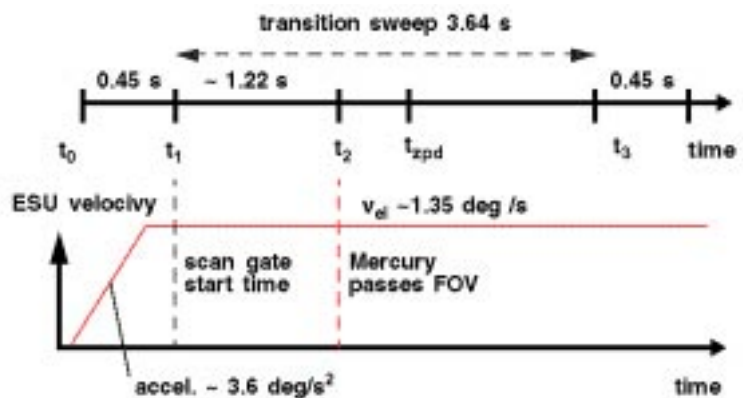


Figure 4 (b).

IF14 timeline and elevation scan unit velocity profile. Note that the actual raw data acquisition starts at the scan gate start time (t_1), whereas the passage of the planet across the FOV occurs ca. 1.22 s later. The effective angular velocity during the passage is approx. 1.29 deg/s.



Therefore, a dedicated in-flight characterisation measurement was included in the calibration/characterisation plan ([3]) in order to provide field-of-view pattern and misalignment information for all 8 detector channels independently.

This particular measurement is based on the acquisition of the detector signals in the raw data mode while the instrument's line-of-sight is actively scanned across an infrared-bright source along the elevation direction. Unlike in the LOS mode, where only detector D1&D2 signals are recorded in the so-called 'total-power' mode, with the interferometer slides fixed in their end positions, the slide mechanism is activated in this measurement, and the optical path difference system provides the trigger signal for sampling all detector outputs synchronously.

For the actual characterisation measurement Mercury has been chosen as a target, because it provides sufficient photon flux across all MIPAS spectral bands and provided observation opportunities in the appropriate geometry during the available measurement period.

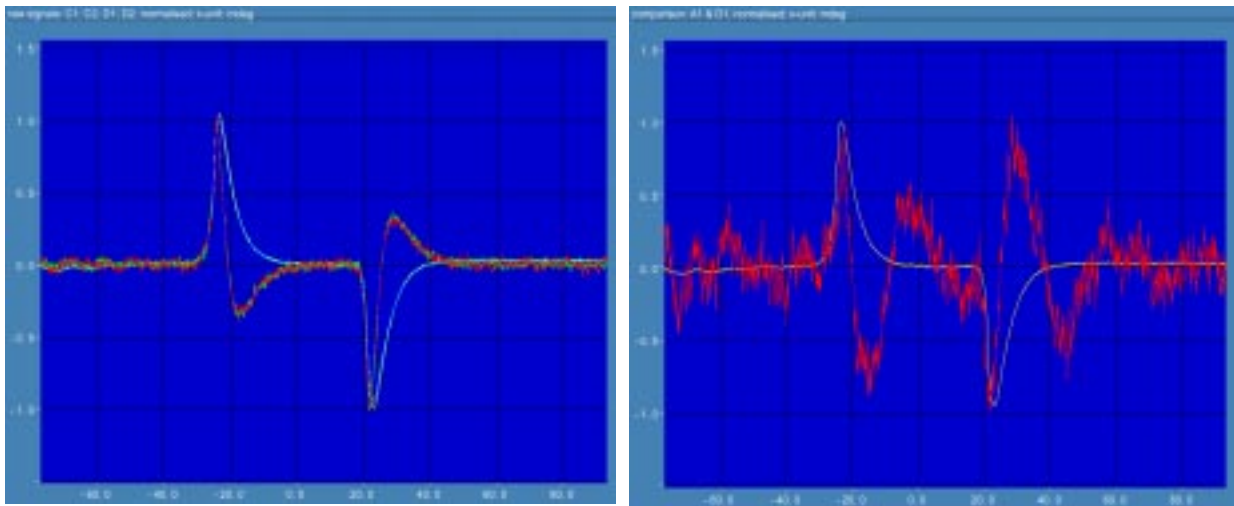
The analysis of the IF 14 measurement is based on a direct comparison of the individual detector signals. Given a sampling rate in the raw data mode of 76066 samples/s and an effective, constant angular velocity of the planet source of 1.29 deg/s an 'angular' sampling in the elevation direction of approx. 17 μ deg/sample is achieved.

Two examples of raw signals are shown in Figure 5, which show overplots of the outputs of detector groups (C1, C2, D1, D2) and (A1, D1), respectively. As in the case of the LOS measurements a 'derivative' type signal is obtained for each detector, due to the AC coupling between detector outputs and pre-amplifiers (note that the 'noisier' signals in each plot correspond to the lower frequency channels; e.g., the red curve in right hand plot represents channel A1).

Because of the different analogue response characteristics (especially near the low frequency cut-off) the observed signal shapes vary between individual detectors. However, due to the high temporal (and thus angular) resolution of the data acquisition the position of the FOV edges and of the 'points of deflection', POI, can be accurately determined. The latter correspond to the positions of positive and negative maxima in the raw signals.

Figure 5. FOV check measurements for detector groups C1, C2, D1, D2 (left plot) and A1, D1 (right plot).

- Notes:
1. signal amplitudes have been normalised to maximum value for each detector
 2. x-axis has been re-scaled using an assumed angular sampling rate of 17 mdeg/s, the zero offset is arbitrary



A comparison of the POI positions yields:

$$C1 \ \& \ C2: \quad POI_{\text{left/right}} = -23.8 \text{ mdeg} / +21.8 \text{ mdeg}$$

$$D1 \ \& \ D2: \quad POI_{\text{left/right}} = -23.4 \text{ mdeg} / +23.1 \text{ mdeg}$$

for other detectors (not all shown in plot):

$$A1 \ \& \ A2: \quad POI_{\text{left/right}} = -23.3 \text{ mdeg} / +21.7 \text{ mdeg}$$

$$B1 \ \& \ B2: \quad POI_{\text{left/right}} = -23.5 \text{ mdeg} / +21.9 \text{ mdeg}$$

In summary, it can be concluded that POI positions coincide within ~ 1.3 mdeg for all 8 detector channels. Furthermore, no evidence for a relative misalignment of FOV patterns of individual detectors or for asymmetries is found.

Analysis tools

Most calibration measurements acquired during the initial 6 months of MIPAS in-orbit operation have been analysed on the MICAL platform, using a suit of specifically designed algorithm chains and additional supporting tools (e.g., IDL). Essential software components have been developed by ABB BOMEM Inc., in the frame of ESA contracts ([7])

Additionally, independent analyses will be carried out by ESA external expert teams (see also Table 1). The status of these still ongoing activities and first results will be reported in separate papers ([8]).

5 SUMMARY / CONCLUSIONS

Following the initial switch-on on 24 March 2002 the MIPAS instrument has undergone a large number of functional checks and dedicated performance measurements. In the course of the data analysis the instrument's health and full functionality in all spectral bands could be verified. Essential parameters, in particular related to radiometric and spectral performance, LOS mispointing and overall stability, have been re-characterised in flight and - if possible - compared to pre-launch characterisation results (FM). Primary performance parameters were found within specifications or in line with pre-launch predictions. The impact of characterisation inaccuracies on radiometric errors as well as long-term changes in the overall radiometric response, e.g. due to ice deposition in the cooled focal-plane subsystem, require further analyses.

ACKNOWLEDGEMENTS

The authors are grateful to all teams and engineers involved in the MIPAS SODAP activities and in the instrument calibration & characterisation project, in particular R. Gessner (Astrium GmbH) and G. Aubertin (ABB BOMEM). Special thanks to J.C. Debruyne (ESTEC) for his engagement in MIPAS s/w projects and the data management, M. Endemann (ESTEC) for many fruitful discussions, and to B. Duesmann (ESTEC), who was involved in the definition and verification of the MIPAS planning tools. Thanks also to A. O'Connell (now with Eumetsat), D. Patterson and F. Diekmann (ESOC) who have been operating the instrument during initial switch-on and commissioning phase.

REFERENCES

- [1] "The MIPAS Science Report", ESA Publication SP-1229, ISBN-no. 92-9092-512-4, March 2000
- [2] Endemann, M. et al., "MIPAS, An Instrument for Atmospheric Chemistry and Climate Research", ESA Bulletin No. 101, ISBN-no. 0376-4265
- [3] Nett, H., "Implementation of MIPAS Post-Launch Calibration and Validation Tasks", PO-PL-ESA-GS-1124, issue 1 B
- [4] Fortin, S. Moreau, "In-Flight Characterisation and Calibration Definition", PO-TN-BOM-GS-0013, issue 1 B
- [5] Lachance, R.L., "MIPAS Level 1B Algorithm Technical Baseline Document", PO-TN-BOM-GS-0012, issue 1 A
- [6] Burgess, A. et al., "Spectral Characterisation and Calibration of MIPAS", ENVISAT Calibration Review, 9-13 September 2002 (to be published in proceedings)
- [7] ESA contracts 12303/96/NL/GS and 15504/01/NL/SF
- [8] Perron, G., "MIPAS Line-Of-Sight Calibration Algorithm", PO-RP-BOM-GS-0008, issue 1 D
- [9] results of MIPAS CalVal activities / independent data analyses, ENVISAT Calibration Review, 9-13 September 2002 (to be published in proceedings)